Journal of Saffron Research
Vol. 13, No. 2, p. 353- 367, 2025
10.22077/jsr.2026.11019.1301

University of Birjand

Original Article

Mapping Saffron Cultivation Areas Using Landsat 8-9 Time-Series and a Pixel-Based SVM Classification Method

Milad Janalipour[1], Nadia Abbaszadeh Tehrani[2], Mohammad Jafari[3]

1- Aerospace Research Institute, Ministry of Science Research and Technology, Tehran, Iran.
2- Aerospace Research Institute, Ministry of Science Research and Technology, Tehran, Iran.
3- Remote Sensing and Geographic Information System, Islamic Azad University, Tehran, Iran.

*Corresponding author: *milad_janalipour@ari.ac.ir*

Received: 19 February 2026; **Revised:** 23 March 2026, **Accepted:** 26 April 2026

Abstract

Remote sensing provides an efficient and cost-effective way to estimate the cultivation area of agricultural crops. In this study, the cultivation area of saffron in Roshtkhar city was estimated using Landsat 8 and 9 time-series imagery and a pixel-based Support Vector Machine (SVM) classification method. The analysis, conducted for the Persian calendar year 1402 (2023 AD), identified approximately 450 hectares of saffron cultivation. An accuracy assessment indicated that the proposed method performed robustly. Based on test samples, classification of Landsat 8 imagery yielded an overall accuracy of approximately 92% and a user's accuracy of 95% for the saffron class. Results from Landsat 9 imagery were similarly high, with an overall accuracy of roughly 91% and a saffron class accuracy ranging from 90% to 93%. Consequently, while Landsat 8 demonstrated slightly superior performance in identifying saffron lands, both sensors proved highly effective for this application, confirming the suitability of the proposed method for distinguishing saffron from other land cover classes.

Conflict of interests: No conflicts of interest are declared by the authors.

Keywords: Machine Learning, Precision Agriculture, Remote Sensing, Saffron.

Introduction

The increasing global population and the need to ensure food security have further highlighted the importance of precise monitoring and optimal management of agricultural resources (Kouzegaran et al., 2013). In this context, the accurate estimation of crop cultivation area, especially for high-value and strategic crops such as saffron, plays a key role in economic planning, market policies, and water resource management. In Iran, the estimation of agricultural crop areas is typically conducted through three main approaches: expert estimation, census-based surveys, and the use of new technologies, including Remote Sensing (RS) and Geospatial Information Systems (GIS) (Farzadmehr & Tabaki Bajestani, 2018). Traditional methods of data collection, based on field surveys, are often costly, time-consuming, and sometimes prone to human error. Consequently, RS technology has emerged as a powerful, accurate, cost-effective, and rapid tool for monitoring crop cultivation area over large scales (Janalipour & Taleai, 2017). Today, various sensors designed for natural resource and agricultural studies are operating on satellites launched into space, collecting terrestrial data from the Earth's surface (Rahdary et al., 2013). Various countries and organizations have used satellite data and different analytical methods for area estimation (Kussul et al., 2012).

RS technology operates based on the reflection of electromagnetic waves from vegetation. Healthy vegetation, due to the presence of chlorophyll and the internal structure of leaves, absorbs visible light and strongly reflects near-infrared (NIR) light. This unique spectral characteristic forms the foundation for developing vegetation indices. The use of RS for identifying and classifying agricultural crops dates back several decades. Early research primarily focused on extensive crops such as wheat (Abbaszadeh et al., 2011; Kamali et al., 2018), corn, and rice. Agilandeeswari et al (2022) presented a crop classification method for hyperspectral images using a partition based band selection approach. The hyperspectral cube is divided into visible, NIR, and shortwave infrared regions based on plant biophysical properties. Bands are selected from each region using entropy, the Normalized Difference Vegetation Index, and the Modified Normalized Difference Water Index respectively. A two-dimensional convolutional neural network is then trained with the selected bands for classification. Experiments on Indian Pines and Salinas datasets show high accuracy for corn, soybean, fallow, and lettuce crops, outperforming several existing methods (Agilandeeswari et al., 2022). Kussul et al (2017) proposed a deep learning architecture for land cover and crop type classification using multi-temporal images from Landsat 8 and Sentinel-1A satellites. The method consists of four levels including preprocessing with self-organizing maps for cloud removal, supervised classification, post-processing, and geospatial analysis. For classification, an ensemble of convolutional neural networks is applied and compared with random forest and an ensemble of multilayer perceptrons. Experiments on a test site in Ukraine show that the ensemble of two dimensional convolutional neural networks achieves the highest overall accuracy at 94.6 % and successfully discriminates summer crops such as maize and soybeans with accuracies above 85 percent (Kussul et al., 2017). Siachalou et al., (2015) proposed a crop classification approach using Hidden Markov Models to link crop phenology with time series of multi-sensor satellite data. The method models the dynamic growth stages of crops as hidden states, which are inferred from a sequence of RS observations. The study evaluates different combinations of RapidEye and Landsat ETM+ images over a heterogeneous agricultural area in Greece with small sized fields. Results show that

using four pan sharpened Landsat ETM+ images together with one RapidEye image achieves the highest overall accuracy of 89.7 percent. The approach effectively discriminates major crop types including cotton, rice, sugar beet, alfalfa, maize, and wheat by exploiting their phenological differences throughout the growing season (Siachalou et al., 2015).

While extensive research has focused on mapping major crops like wheat and corn using medium-resolution imagery, the RS of minor yet high-value crops such as saffron presents unique challenges. Previous studies have successfully discriminated various land cover classes, but they often rely on dense vegetation cover or distinct spectral signatures during peak growing seasons. Saffron, however, exhibits atypical phenological characteristics; its sparse canopy cover during the growing season results in a significant contribution of background soil to the pixel reflectance, complicating its spectral identification. Furthermore, the smallholder nature of saffron farming, particularly in regions like Iran, leads to fragmented fields that are often below the pure-pixel resolution of many sensors, and are frequently intercropped with permanent crops like pistachios. Therefore, a gap remains in developing methodologies specifically tailored to detect such spectrally and spatially complex targets.

With advancements in the spatial and spectral resolution of sensors, it has become possible to detect crops with smaller cultivation areas and specific growth patterns, such as saffron. In a study by Sishodia et al., (2020), in a systematic review, concluded that machine learning and object-based algorithms have now become a standard for precise agricultural crop classification (Sishodia et al., 2020).

Few studies have been conducted on the identification and discrimination of saffron and pistachio crops. The separation of these two crops based on Landsat time-series imagery has not been reported yet. Additionally, a sensitivity analysis of the results with respect to SVM parameters has not been addressed in previous research. While previous crop-classification studies have often relied on either high-resolution single-date imagery or conventional classifiers without rigorous optimization, this study introduces a novel approach by integrating Landsat 8-9 time-series data with a pixel-based SVM classification. The key novelty lies not only in the application of this combination to the specific case of saffron and pistachio mapping, but also in the comprehensive sensitivity analysis of the SVM parameters. This sensitivity analysis, which is largely overlooked in prior crop-classification efforts, allows for a deeper understanding of model behavior and ensures the robustness and reliability of the classification results. This combined framework offers a replicable methodology for accurately discriminating complex crop types.

Materials and Methods

Study Area:

Roshtkhar city was selected as the study area due to its prominent role as a major saffron-producing region in Razavi Khorasan Province, where saffron cultivation forms the backbone of the local agricultural economy (Asghari Lafmejani & Eizadi, 2017; Izadi & Asghari Lafmejani, 2023). The region is characterized by a complex landscape of smallholder farms where saffron fields are often interwoven with pistachio orchards, making traditional area estimation methods inaccurate and time-consuming. Therefore, achieving an accurate and timely estimation of saffron cultivated area in this specific region is crucial for improving agricultural management, supporting food security policies, and optimizing resource allocation for local farmers.

Roshtkhar city, with an area of approximately 4,360 km^2, is located in Razavi Khorasan Province, Iran. The county is bounded to the north and west by Torbat-e Heydariyeh, to the southeast

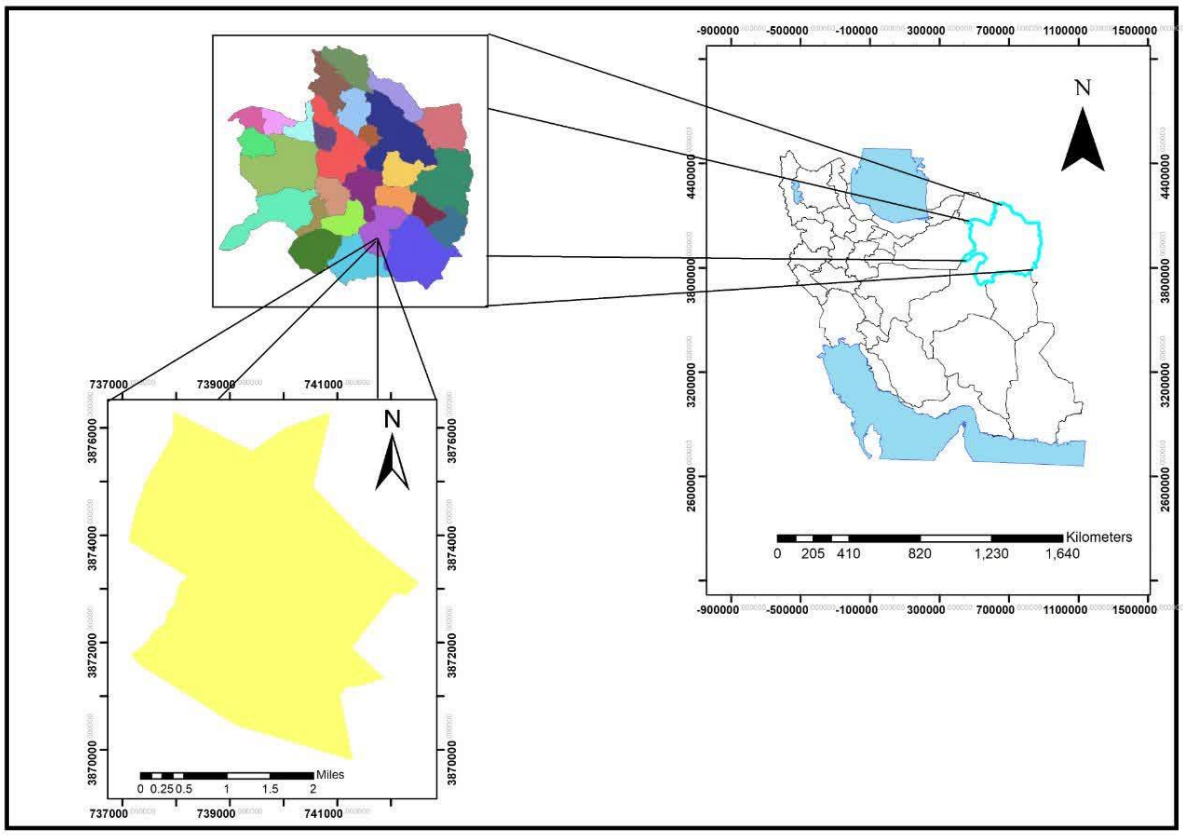

Fig. 1. Location of the study area (Roshtkhar city)

by Khaf County, and to the south by Gonabad County. The county comprises two central districts (Markazi and Jangal) and four rural districts (Roshtkhar and Astaneh in the central district, and Jangal and Shobeh in the Jangal district) (Shatri et al., 2023). The study area is shown in Fig. 1.

Data Used:

Landsat 8 and 9 satellite images from the United States Geological Survey (USGS) website, with Path 159 and Row 36, were used to estimate the cultivation area of saffron. Table 1 shows the acquisition dates of the images from Landsat 8 and 9 satellites.

To encompass a complete annual growth cycle for both saffron and pistachio, all available Landsat 8 and 9 images from March 2022 to March 2023 were considered for analysis. From this archive, only scenes with less than 20% cloud cover were selected to ensure data quality and temporal consistency. This one-year timeframe was deliberately chosen because the phenological cycles of saffron (a winter crop) and pistachio (a perennial tree crop) are distinctly separable within a single growing season, allowing for accurate discrimination between the two crop types.

Field samples were collected in two independent stages from different location within the study area. Due to the larger number of samples obtained in the first stage, these samples were used as the training dataset, while the samples collected during the second stage were used as the testing dataset. To generate reliable training and test data for the supervised classification, a two-step ground data collection strategy was employed. First, for the agricultural classes (saffron and pistachio), extensive field surveys were conducted across the study area using a handheld GPS device. To enhance the spatial accuracy of the collected samples, the boundaries (polygons) of the surveyed fields were

carefully reviewed and refined against very high-resolution imagery available in Google Earth Pro. This process ensured that the training pixels accurately represented pure stands of each crop and minimized mixed-pixel effects. Second, for the non-agricultural classes (urban areas and bare soil), training samples were directly digitized as polygons in Google Earth Pro, leveraging its high-resolution archival imagery for precise delineation. These polygons were then converted into shape-files. The number and location of extracted polygons are presented in Table 2 and Fig. 2.

Test polygons were also collected through field surveys using GPS and Google Earth Pro software. They were subsequently converted into shapefiles. The test dataset was kept independent of the training data and is used for classification accuracy assessment. The number of test polygons is presented in Table 3 and Fig. 3.

Table 1. Landsat 8 and 9 satellite images used in this study

Landsat 8 Images		**Landsat 9 Images**	
Image No.	**Solar Date**	**Image No.**	**Solar Date**
Image 1	1401/12/24	Image 1	1401/12/17
Image 2	1402/01/06	Image 2	1401/12/20
Image 3	1402/01/23	Image 3	1401/12/22
Image 4	1402/01/29	Image 4	1401/12/23
Image 5	1402/02/19	Image 5	1402/02/25
Image 6	1402/03/23	Image 6	1402/02/21
Image 7	1402/05/12	Image 7	1402/03/11
Image 8	1402/05/21	Image 8	1402/03/23
Image 9	1402/06/04	Image 9	1402/04/08
Image 10	1402/06/21	Image 10	1402/04/24
Image 11	1402/07/10	Image 11	1402/05/10
Image 12	1402/07/25	Image 12	1402/05/25
Image 13	1402/08/10	Image 13	1402/06/10
Image 14	1402/10/11	Image 14	1402/06/26
		Image 15	1402/07/11
		Image 16	1402/07/27
		Image 17	1402/08/29
		Image 18	1402/09/15
		Image 19	1402/10/01

Table 2. Number of extracted polygons used for training machine learning methods

Land Cover/Feature Class	**Number of Polygons**	**Number of pixels**
Pistachio	61	237
Urban	33	196
Saffron	106	237
Bare soil	40	178

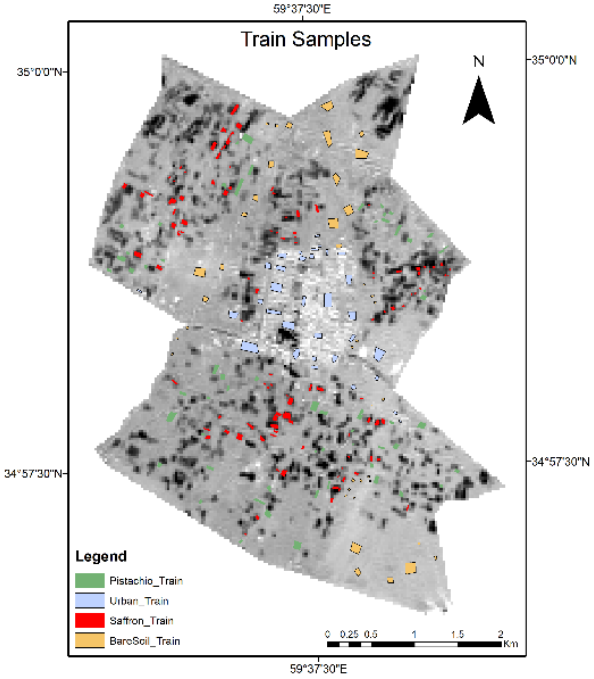

Fig. 2. Ground truth training polygons

Table 3. Number of test polygons used in this study

Land Cover/Feature Class	Number of Polygons	Number of pixels
Pistachio	37	165
Urban	19	127
Saffron	54	82
Bare soil	34	124

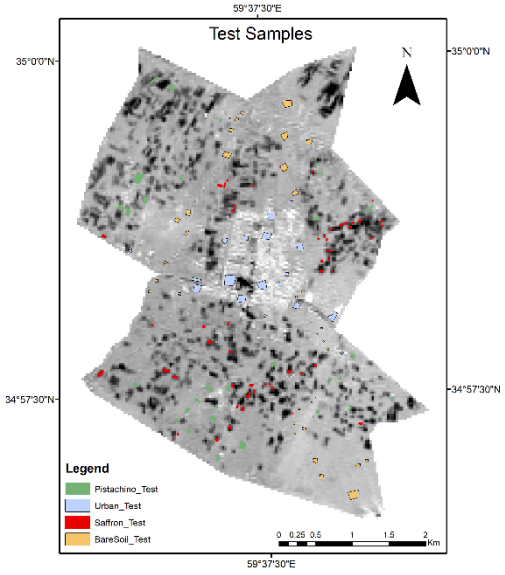

Fig. 3. Ground truth test polygons

Proposed Method:

All steps of the proposed method were applied in ENVI software. Initially, Landsat 8 and 9 satellite images covering the 1401-1402 (2022-2023) agricultural season for the study area were downloaded from the USGS website. Subsequently, field visits were conducted to collect training and test (control) samples from the study area. A Geographic Information System (GIS) was employed to produce classification maps and estimate the cultivation area. The required information for this research was gathered through a literature review and field study methods. The selection of Landsat imagery was based on its relatively suitable spatial and temporal resolution, free and open availability, and its temporal distribution aligning well with the agricultural crop growth cycle (Abiyat, 2022).

In the next step, field sampling of training and test samples was performed using GPS, and the study area was clipped from the satellite images based on the county boundary. Subsequently, to enhance image quality, radiometric and atmospheric corrections were applied to the images (Abbaszadeh Tehrani et al., 2025).

The Green Normalized Difference Vegetation Index (GNDVI) was calculated across all time points, then stacked with a single-time Normalized Difference Built-Up Index (NDBI) layer and used as input for classification. Classification was performed on the selected indices i.e., the integration of GNDVI time-series and NDBI using a pixel-based method. The prepared samples were used for validation, and based on the results of the method, the cultivation area of saffron was estimated (Giovos et al., 2021).

Preprocessing: To improve image quality, enhance clarity, and consequently increase the amount of extractable information, radiometric and atmospheric corrections were applied to the images (Abbaszadeh Tehrani et al., 2025). When using satellite images to study and analyze terrestrial features and phenomena, it is sometimes necessary to remove the atmospheric contribution to the reflectance values of features within the image (Ahern et al., 1987; Kobayashi & Sanga-Ngoie, 2008). For the atmospheric correction of Landsat 8 and 9 images, the QUAC (Quick Atmospheric Correction) algorithm was used. This algorithm utilizes visible and NIR bands for atmospheric correction. The QUAC algorithm is an approximation of the FLAASH atmospheric correction and provides surface reflectance with appropriate accuracy (Liu et al., 2022).

Satellite Image Classification Methods: Generally, there are two main approaches for classifying satellite images:

Pixel-Based Methods: These are the oldest and simplest methods, where each pixel is classified independently based on its spectral values across different bands. The Maximum Likelihood (ML) algorithm, which was also used in this study, is a popular parametric statistical method in this category. This algorithm assumes that the data distribution within each class follows a normal distribution and assigns a pixel to the class to which it has the highest probability of belonging (Hussain et al., 2013; Zerrouki & Bouchaffra, 2014).

Object-Based Methods: In these methods, the image is first segmented into homogeneous segments or objects. These objects are then classified based on various criteria such as average spectral value, texture, shape, and context. Due to their use of spatial information and reduction of the "salt-and-pepper" effect in the final map, these methods hold significant advantages over pixel-based methods, especially in areas with small agricultural plots (Blaschke, 2010; Walter, 2004).

In addition to classical methods, powerful machine learning algorithms are widely used in remote sensing. The algorithm

employed in this research is SVM. This algorithm is a non-parametric classifier that seeks to find the optimal hyperplane to separate classes in feature space. SVM handles high-dimensional data and small training sample sizes well and has demonstrated superior performance compared to the Maximum Likelihood algorithm in many studies, including agricultural applications.

SVMs are a group of supervised machine learning classification algorithms based on statistical learning theory that have been applied in the field of remote sensing (Foody & Mathur, 2006). The foundations of SVMs were developed by Vapnik (Gunn, 1998) and have gained significant popularity due to their many attractive features and promising empirical performance. SVM is a popular method for classification and regression in machine learning and data mining (Vapnik, 2013). SVMs are particularly attractive in the field of remote sensing due to their ability to successfully manage small training datasets, which often yield higher classification accuracy than traditional methods (Mantero et al., 2005).

We performed an exhaustive grid search to tune the SVM parameters. The Gamma parameter was searched over the range [0.05, 0.5, 1, 10, 50, 100, 200, 400, 600, 800, 1000], and the penalty parameter C was searched over the range [0.05, 0.5, 1, 10, 50, 100, 200, 400, 600, 800, 1000]. This optimization procedure was performed independently for Landsat-8 and Landsat-9 datasets using the same validation protocol to account for potential sensor-specific variations.

Validation:

To assess the accuracy and validate the results of the classification, an error matrix (confusion matrix) was employed as the fundamental tool for accuracy assessment. From this matrix, several quantitative metrics were derived. The overall accuracy was calculated, representing the proportion of correctly classified samples relative to the total number of samples. To provide a per-class assessment of the classification performance, the producer's accuracy and the user's accuracy were computed. Finally, to account for the agreement occurring by chance a limitation of overall accuracy which only utilizes the diagonal elements of the matrix the Cohen's Kappa coefficient was calculated. This coefficient measures the agreement between the classified data and the reference data, providing a robust measure of classification reliability (Babaei et al., 2021; Congalton & Green, 2019).

A Radial Basis Function (RBF) kernel was used for performing SVM classification on Landsat 8 and 9 images (Fig. 4). Areas colored in red represent saffron cultivation zones. Pistachio orchards are shown in green and urban areas are delineated in gray.

Results and Discussion

In this study, control samples were used to evaluate the accuracy of the SVM classification. To ensure the reliability of the classification results, accuracy was assessed using the parameters of Overall Accuracy, Kappa Coefficient, Producer's Accuracy, and User's Accuracy. The confusion matrix, overall accuracy, and Kappa coefficient for the Landsat 8 image are presented in Table 4, and for Landsat 9 in Table 5.

Beyond the overall accuracy values, the confusion matrix reveals several patterns that help explain the classification errors. The saffron class achieved relatively high producer’s and user’s accuracies (both about 95%), indicating that most saffron fields were correctly identified and that few pixels labeled as saffron actually belong to other classes. However, a small degree of confusion occurred mainly with pistachio and, to a lesser extent, with urban areas.

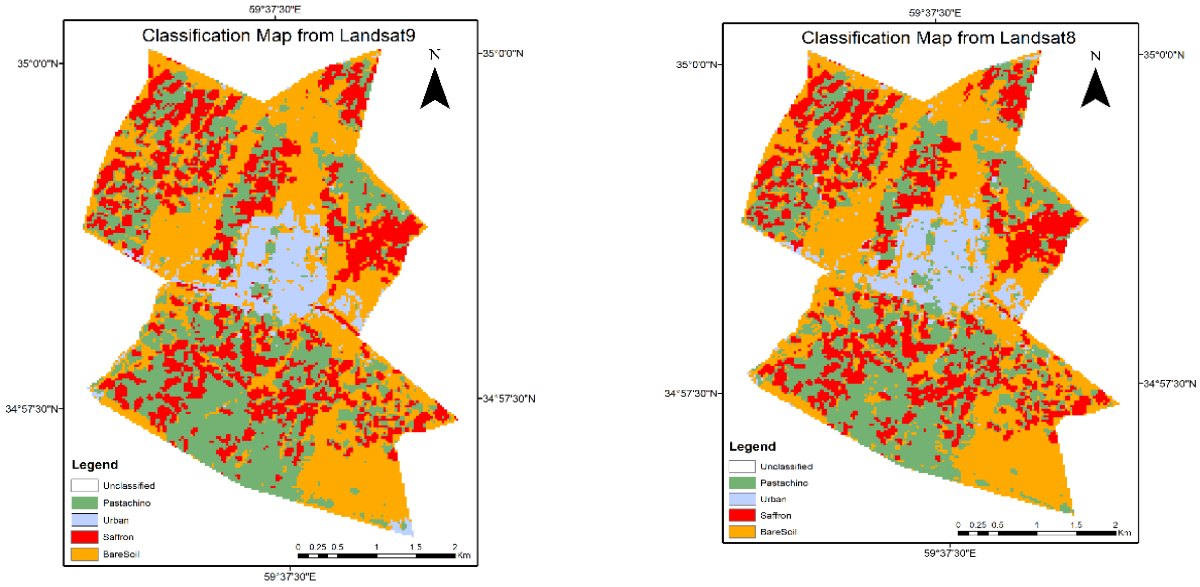

Fig. 4. Maps classified from SVM in 2023 a) Landsat9, b) Landsat8

The confusion between saffron and pistachio can be attributed to similarities in their spectral and temporal characteristics. In the study region, saffron fields often have sparse vegetation cover for a large portion of the year, and their spectral response is strongly influenced by exposed soil. Similarly, pistachio orchards may exhibit low canopy density, especially in younger orchards or during certain phenological stages, which increases the contribution of soil background in satellite observations. This similarity can lead to occasional misclassification between these two classes even when time-series features are used.

Some confusion is also observed between bare soil and urban areas, as well as between bare soil and pistachio. This is likely related to the spectral resemblance between dry soil surfaces and certain urban materials, particularly in medium-resolution imagery where mixed pixels are common. In addition, agricultural fields that are temporarily fallow may appear spectrally similar to bare soil.

Overall, although the classification accuracy is high, the remaining errors are largely associated with spectral similarity, sparse vegetation structure, and mixed-pixel effects in the study area. These factors are common challenges in crop mapping using medium-resolution satellite data and explain the limited but persistent confusion between saffron and pistachio classes. In the SVM classification for the Landsat 8 image, out of a total of 83 reference pixels for saffron, 79 pixels were correctly classified as saffron, 3 pixels were misclassified as pistachio, and 1 pixel was misclassified as urban.

Table 4. Confusion matrix for Landsat 8 image using the SVM method

Class	Urban	Saffron	Bare Soil	Pistachio	Total	User's Acc. (%)	Producer's Acc. (%)
Urban	118	1	6	0	125	94.40%	86.76%
Saffron	1	79	0	3	83	95.18%	95.18%
Bare Soil	13	1	114	5	133	85.71%	94.21%
Pistachio	4	3	1	149	157	94.90%	94.30%
Total	136	83	121	158	498		

Table 5. Confusion matrix for Landsat 9 image using the SVM method

Class	Urban	Saffron	Bare Soil	Pistachio	Total	User's Acc. (%)	Producer's Acc. (%)
Urban	115	1	3	0	118	97.46%	84.56%
Saffron	1	76	1	4	82	92.68%	91.57%
Bare Soil	15	1	116	5	137	84.67%	95.87%
Pistachio	5	6	1	149	161	92.55%	94.30%
Total	136	83	121	158	498		

The Producer's Accuracy for the saffron class is 95.18 percent, and the User's Accuracy is 95.18 percent. The Overall Accuracy is 92.36%, and the Kappa coefficient is 0.8967.

In the SVM classification for the Landsat 9 image, out of a total of 83 reference pixels for saffron, 76 pixels were correctly classified, 4 pixels were misclassified as pistachio, 1 pixel as barren land, and 1 pixel as urban. The Producer's Accuracy for saffron is 91.57 percent, and the User's Accuracy is 92.68 percent. The Overall Accuracy is 91.56%, and the Kappa coefficient is 0.8858.

Following the initial classification, attempts were made to improve the method by tuning the Gamma and Penalty (C) parameters. The results of this sensitivity analysis are presented in Table 6 (for Landsat 8) and Table 7 (for Landsat 9). In these experiments, the values of Gamma and Penalty (C) were varied from 0.05 to 1000. For each combination, the classification was executed and validated. The overall accuracy values ranged from 79 percent to 93 percent, indicating the significant influence of these parameters on the output. The Penalty (C) parameter had the greatest impact, with the best results for Landsat 8 achieved at a value of 400.

Based on the results obtained, the Penalty (C) parameter had the most significant impact on accuracy. The highest overall accuracy for Landsat 9 was 91.96 percent, achieved at Penalty (C) values of 600 and 1000.

Although Landsat 8 showed slightly higher classification accuracy than Landsat 9, the difference in performance between the two sensors was relatively small. This result indicates that both sensors provide comparable spectral and temporal information for saffron mapping. Since Landsat 8 and Landsat 9 have very similar sensor characteristics, spectral bands, and spatial resolution, their classification capabilities are expected to be largely consistent. From a practical perspective, the small difference in performance suggests that either dataset can be reliably used for saffron monitoring and land-cover classification in the study area. Moreover, the compatibility between the two sensors enables their combined use to increase temporal coverage and reduce data gaps caused by cloud cover or acquisition intervals. Integrating observations from both Landsat 8 and Landsat 9 can therefore improve the availability of time-series data and support more continuous agricultural monitoring without significantly affecting classification reliability.

After determining the map with the highest accuracy, it was used to estimate the saffron cultivation area. The extracted saffron cultivation area from the SVM classification for Landsat 8 is 450.40 hectares, and for Landsat 9, it is 458.54 hectares. Fig. 5 presents the spatial distribution maps of saffron cultivation derived from Landsat 8 and Landsat 9 using the SVM method.

The combination of GNDVI time-series with a single-date NDBI layer was selected to enhance the separability between saffron and other land-cover classes by incorporating both vegetation dynamics and built-up surface information. GNDVI is particularly sensitive to chlorophyll content and

vegetation vigor, making it suitable for capturing phenological changes in crops over time. Since saffron has a distinctive growth cycle characterized by a short vegetative period and long intervals of low vegetation cover, its temporal GNDVI profile differs from many other land-cover types. The use of a time-series therefore helps capture these seasonal dynamics and improves discrimination from crops or vegetation types with different phenological patterns.

In addition to vegetation information, the NDBI layer was included to help distinguish non-vegetated surfaces, particularly urban areas and built-up land, which may occasionally exhibit spectral similarity to sparsely vegetated agricultural fields. By highlighting built-up features, NDBI provides complementary information that reduces confusion between saffron fields during their low-vegetation stages and nearby urban surfaces.

Table 6. Overall accuracy of the SVM classifier relative to changes in Gamma and Penalty (C) parameters on Landsat 8 images

1000	800	600	400	200	100	50	10	1	0.5	0.05	Gamma
											penalty
79.31	79.31	79.31	79.31	79.31	79.31	79.31	79.31	79.31	79.31	79.31	**0.05**
82.32	82.32	82.32	82.32	82.32	82.32	82.32	82.32	82.32	82.32	82.32	**0.5**
80.32	80.32	80.32	80.32	80.32	80.32	80.32	80.32	80.32	80.32	80.32	**1**
86.14	86.14	86.14	86.14	86.14	86.14	86.14	86.14	86.14	86.14	86.14	**10**
91.36	91.36	91.36	91.36	91.36	91.36	91.36	91.36	91.36	91.36	91.36	**50**
92.36	92.36	92.36	92.36	92.36	92.36	92.36	92.36	92.36	92.36	92.36	**100**
93.57	93.57	93.57	93.57	93.57	93.57	93.57	93.57	93.57	93.57	93.57	**200**
93.57	93.57	93.57	93.57	93.57	93.57	93.57	93.57	93.57	93.57	93.57	**400**
93.37	93.37	93.37	93.37	93.37	93.37	93.37	93.37	93.37	93.37	93.37	**600**
92.97	92.97	92.97	92.97	92.97	92.97	92.97	92.97	92.97	92.97	92.97	**8000**
92.97	92.97	92.97	92.97	92.97	92.97	92.97	92.97	92.97	92.97	92.97	**1000**

Table 7. Overall accuracy of the SVM classifier relative to changes in Gamma and Penalty (C) parameters on Landsat 9 images

1000	800	600	400	200	100	50	10	1	0.5	0.05	Gamma
											penalty
74.89	74.89	74.89	74.89	74.89	74.89	74.89	74.89	74.89	74.89	74.89	**0.05**
79.71	79.71	79.71	79.71	79.71	79.71	79.71	79.71	79.71	79.71	79.71	**0.5**
80.12	80.12	80.12	80.12	80.12	80.12	80.12	80.12	80.12	80.12	80.12	**1**
85.54	85.54	85.54	85.54	85.54	85.54	85.54	85.54	85.54	85.54	85.54	**10**
91.36	91.36	91.36	91.36	91.36	91.36	91.36	91.36	91.36	91.36	91.36	**50**
91.53	91.53	91.53	91.53	91.53	91.53	91.53	91.53	91.53	91.53	91.53	**100**
91.56	91.56	91.56	91.56	91.56	91.56	91.56	91.56	91.56	91.56	91.56	**200**
91.56	91.56	91.56	91.56	91.56	91.56	91.56	91.56	91.56	91.56	91.56	**400**
91.96	91.96	91.96	91.96	91.96	91.96	91.96	91.96	91.96	91.96	91.96	**600**
91.76	91.76	91.76	91.76	91.76	91.76	91.76	91.76	91.76	91.76	91.76	**800**
91.96	91.96	91.96	91.96	91.96	91.96	91.96	91.96	91.96	91.96	91.96	**1000**

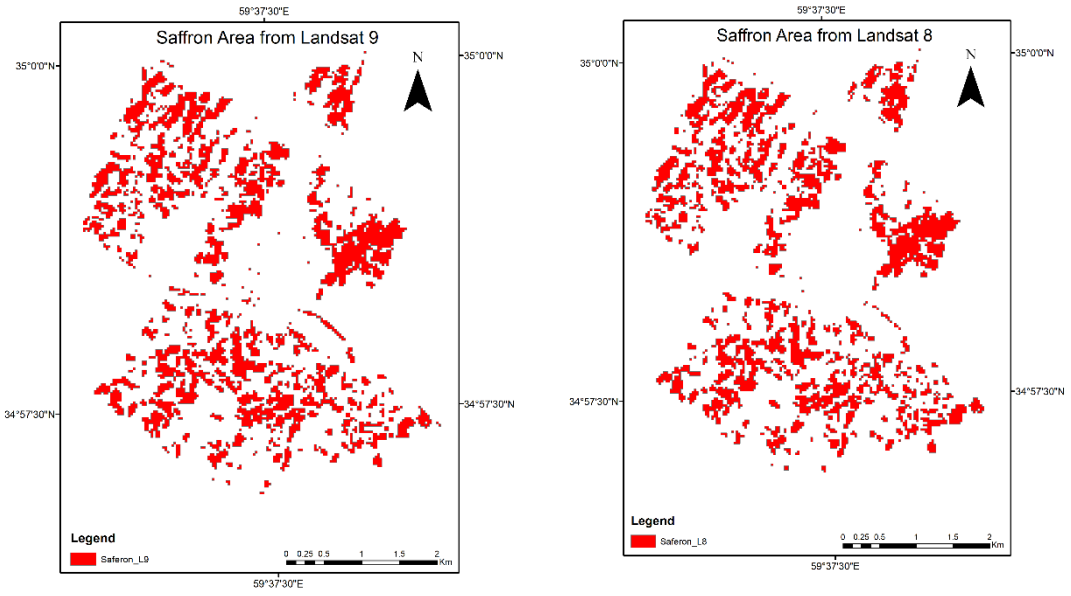

Fig. 5. Distribution map of saffron cultivated land in 2023 from a) Landsat 9 and b) Landsat 8 using the SVM method.

Therefore, the integration of temporal vegetation indices (GNDVI) with a structural indicator of built-up areas (NDBI) was expected to improve the overall separability among saffron, pistachio orchards, bare soil, and urban areas in the classification process.

The classification in this study was performed using a pixel-based approach, which classifies each pixel independently based on its spectral and temporal characteristics. While this method is widely used and effective for large-scale land-cover mapping, it may present some limitations when applied to crops such as saffron that are often cultivated in small and fragmented fields. In such cases, the relatively coarse spatial resolution of medium-resolution satellite imagery can result in mixed pixels, where a single pixel contains a combination of different land-cover types. This effect may contribute to some of the observed misclassifications.

An alternative approach is object-based image analysis (OBIA), where groups of pixels are segmented into meaningful objects before classification. This method can incorporate additional spatial characteristics such as shape, texture, and contextual relationships, which may improve the discrimination of fragmented agricultural fields.

Despite these potential advantages, the pixel-based method was selected in this study because of its simplicity, lower computational requirements, and its suitability for handling multi-temporal satellite data. Moreover, the achieved accuracy indicates that the pixel-based approach was sufficiently effective for mapping saffron cultivation at the regional scale. Nevertheless, future studies could explore object-based approaches to further improve classification performance in areas with highly fragmented agricultural patterns.

Despite the satisfactory classification results, several limitations of this study should be acknowledged. First, although the training and test samples were collected carefully, the transparency and size of the sample dataset may influence the robustness of the model. A larger and more systematically distributed sample set could further improve the

representativeness of the training data and reduce potential bias.

Second, the classification scheme included only four land-cover classes, focusing on the dominant and most relevant categories in the study area. While this simplified scheme helped improve class separability, the exclusion of other minor land-cover types may limit the completeness of the land-cover representation.

Another limitation is the potential spatial dependence between some training and test samples. If samples are located close to each other, spatial autocorrelation may slightly inflate the reported accuracy metrics. Future studies could address this issue by applying spatially stratified sampling or spatial cross-validation techniques.

Finally, the study did not explicitly quantify the uncertainty associated with the estimated saffron cultivation area. Although classification accuracy metrics were reported, area-based uncertainty measures or confidence intervals were not calculated. Incorporating uncertainty analysis methods in future research would provide a more comprehensive assessment of the reliability of area estimates derived from satellite-based classification.

Conclusion

The aim of this research was to determine the cultivation area of saffron in Roshtkhar city, using Landsat 8 and 9 time-series imagery and a pixel-based SVM classification method. The analysis of Landsat 8 imagery showed that the overall accuracy of the classification for distinguishing agricultural crops was about 92%, while the accuracy of saffron identification reached 95%. The processing of Landsat 9 imagery indicated an overall classification accuracy of approximately 91%, while the accuracy of saffron identification ranged from 90% to 93%. Overall, the findings reveal that the capability of Landsat 8 to detect saffron cultivation was somewhat superior to that of Landsat 9. Furthermore, the cultivation area of saffron in Roshtkhar city was estimated to be 450 hectares. It should be noted that this value represents an estimate derived from satellite-based classification and is therefore subject to uncertainties associated with classification errors, mixed pixels, and the spatial resolution of the imagery. Consequently, the reported area should be interpreted as an approximate indication of the spatial extent of saffron cultivation rather than a fully definitive value.

The parameter sensitivity analysis demonstrated that classification performance is strongly influenced by the selection of model parameters, particularly the Penalty C parameter, with overall accuracy varying noticeably across the tested settings. This finding highlights the importance of systematic parameter optimization when applying machine-learning models for saffron mapping. Future studies should therefore incorporate structured parameter-tuning procedures, such as grid search or cross-validation, to ensure that the selected parameter combinations provide stable and reliable classification results. Careful calibration of model parameters can substantially improve the robustness and transferability of saffron detection methods in different regions and datasets.

For future research, several methodological improvements could further enhance the accuracy of saffron mapping. The integration of Sentinel-2 optical imagery could provide higher spatial resolution and richer spectral information, which may help reduce confusion between saffron, pistachio orchards, and bare soil. In addition, Sentinel-1 radar data could contribute complementary structural and moisture-related information that is less affected by cloud cover and may improve crop discrimination, particularly during periods when optical imagery shows limited spectral differences.

Furthermore, OBIA could be explored as an alternative to the pixel-based approach used in this study. By grouping neighboring pixels into meaningful image

objects and incorporating spatial characteristics such as shape, texture, and contextual relationships, object-based methods may better represent fragmented agricultural fields and reduce mixed-pixel effects. These approaches could potentially address some of the classification uncertainties observed in the present results and lead to more accurate mapping of saffron cultivation areas.

References

Abbaszadeh Tehrani, N., Janalipour, M., & Hosseini, S. B. (2025). Monitoring the urban ecosystem health by introducing a spatial model based on pressure-state-impact-response framework (study area: Sanandaj city). *International Journal of Environmental Science and Technology*, *22*(3), 1751-1768.

ABBASZADEH, T. N., BEHESHTIFAR, M., & Morabi, M. (2011). Crop Type Mapping in Qazvin by Using Multi-Temporal Satellite Images: IRSC-LISSIII DATA.

Abiyat, M. (2022). Evaluation of Efficiency between Classification Methods and Spectral Indices in Cropped Area Estimation of Shush County. *Water and Soil*, *36*(4), 493-509.

Agilandeeswari, L., Prabukumar, M., Radhesyam, V., Phaneendra, K. L. B., & Farhan, A. (2022). Crop classification for agricultural applications in hyperspectral remote sensing images. *Applied Sciences*, *12*(3), 1670.

Ahern, F., Brown, R., Cihlar, J., Gauthier, R., Murphy, J., Neville, R., & Teillet, P. (1987). Review article radiometric correction of visible and infrared remote sensing data at the Canada Centre for remote sensing. *International journal of remote sensing*, *8*(9), 1349-1376.

Asghari Lafmejani, S., & Eizadi, A. (2017). Investigation of saffron role in job creation for rural families (Case study: Roshtkhar Rural District). *Journal of Saffron Research*, *4*(2), 210-228. https://doi.org/10.22077/jsr.2017.521

Babaei, H., Janalipour, M., & Tehrani, N. A. (2021). A simple, robust, and automatic approach to extract water body from Landsat images (case study: Lake Urmia, Iran). *Journal of Water and Climate Change*, *12*(1), 238-249.

Blaschke, T. (2010). Object based image analysis for remote sensing. *ISPRS journal of photogrammetry and remote sensing*, *65*(1), 2-16.

Congalton, R. G., & Green, K. (2019). *Assessing the accuracy of remotely sensed data: principles and practices*. CRC press.

Farzadmehr, J., & Tabaki Bajestani, K. (2018). Capability of Landsat 8 satellite images to estimate the area under cultivation of saffron (case study: city of Torbat Heydarieh). *Saffron Agronomy and Technology*, *6*(1), 49-60. https://doi.org/10.22048/jsat.2017.48518.1194

Foody, G. M., & Mathur, A. (2006). The use of small training sets containing mixed pixels for accurate hard image classification: Training on mixed spectral responses for classification by a SVM. *Remote Sensing of Environment*, *103*(2), 179-189.

Giovos, R., Tassopoulos, D., Kalivas, D., Lougkos, N., & Priovolou, A. (2021). Remote sensing vegetation indices in viticulture: A critical review. *Agriculture*, *11*(5), 457.

Gunn, S. R. (1998). Support vector machines for classification and regression. *ISIS technical report*, *14*(1), 5-16.

Hussain, M., Chen, D., Cheng, A., Wei, H., & Stanley, D. (2013). Change detection from remotely sensed images: From pixel-based to object-based approaches. *ISPRS journal of photogrammetry and remote sensing*, *80*, 91-106.

Izadi, A., & Asghari Lafmejani, S. (2023). The Status of Production of Saffron and Pistachio Currency Converter Products and its Effects in Rural Households (Case Study: Roshtkhwar Rural District). *Journal of Saffron Research*, *11*(2), 250-267. https://doi.org/10.22077/jsr.2023.6418.1215

Janalipour, M., & Taleai, M. (2017). Building change detection after earthquake using multi-criteria decision analysis based on extracted information from high spatial resolution satellite images. *International Journal of remote sensing*, *38*(1), 82-99.

Kamali, L., Kaviani, A., Nazari, B., & Liaghat, A. (2018). Estimation of wheat yield by satellite imageries Landsat 8. *Iranian Journal of Soil and Water Research*, *49*(5), 1031-1042. https://doi.org/10.22059/ijswr.2018.237377.667719

Kobayashi, S., & Sanga-Ngoie, K. (2008). The integrated radiometric correction of optical remote sensing imageries. *International journal of remote sensing*, *29*(20), 5957-5985.

Kouzegaran, S., Mousavi Baygi, M., Sanaeinejad, H., & Behdani, M. A. (2013). Identification relevant areas for saffron cultivation according to precipitation and relative humidity in South Khorasan using GIS.

Journal of Saffron Research, *1*(2), 85-96. https://doi.org/10.22077/jsr.2013.436

Kussul, N., Lavreniuk, M., Skakun, S., & Shelestov, A. (2017). Deep learning classification of land cover and crop types using remote sensing data. *IEEE Geoscience and Remote Sensing Letters*, *14*(5), 778-782.

Kussul, N., Shelestov, A., Skakun, S., Kravchenko, O., & Moloshnii, B. (2012). Crop state and area estimation in Ukraine based on remote and in-situ observations. *Int. J. on Information Models and Analyses*, *1*(3), 251-259.

Liu, S., Zhang, Y., Zhao, L., Chen, X., Zhou, R., Zheng, F., Li, Z., Li, J., Yang, H., & Li, H. (2022). QUantitative and automatic atmospheric correction (QUAAC): application and validation. *Sensors*, *22*(9), 3280.

Mantero, P., Moser, G., & Serpico, S. B. (2005). Partially supervised classification of remote sensing images through SVM-based probability density estimation. *IEEE Transactions on Geoscience and Remote Sensing*, *43*(3), 559-570.

Rahdary, V., Maleki, S., Soffianian, A., Khajeddin, S. J., & Pahlevanravi, A. (2013). Change detection of canopy cover percentage using satellite data during 1972 to 2008 (Case study: Monteh Wild Life Refuge). *Iranian Journal of Range and Desert Research*, *20*(3), 508-521.

Shatri, M., Izadi, A., & Izadi, M. (2023). Consequences of Changing the Pattern of Saffron and Pistachio Cultivation and its Impact on the Development of Rural Areas (Case study: Rashtkhwar city). *Geography and Development*, *21*(72), 178-204. https://doi.org/10.22111/gdij.2023.45065.3503

Siachalou, S., Mallinis, G., & Tsakiri-Strati, M. (2015). A hidden Markov models approach for crop classification: Linking crop phenology to time series of multi-sensor remote sensing data. *Remote Sensing*, *7*(4), 3633-3650.

Sishodia, R. P., Ray, R. L., & Singh, S. K. (2020). Applications of remote sensing in precision agriculture: A review. *Remote Sensing*, *12*(19), 3136.

Vapnik, V. (2013). *The nature of statistical learning theory*. Springer science & business media.

Walter, V. (2004). Object-based classification of remote sensing data for change detection. *ISPRS journal of photogrammetry and remote sensing*, *58*(3-4), 225-238.

Zerrouki, N., & Bouchaffra, D. (2014). Pixel-based or object-based: Which approach is more appropriate for remote sensing image classification? 2014 IEEE International Conference on Systems, Man, and Cybernetics (SMC).